Colloid Polym Sci 277:325–333 (1999)

ORIGINAL CONTRIBUTION

S. Tang
C.M. McFarlane
G.C. Paul
C.R. Thomas

Characterising latex particles and fractal aggregates using image analysis

Received: 28 September 1998
Accepted: 29 October 1998

S. Tang (✉) · C.M. McFarlane
G.C. Paul · C.R. Thomas
Centre for Bioprocess Engineering
School of Chemical Engineering
University of Birmingham
Birmingham B15 2TT, UK
e-mail: s.tang@bham.ac.uk

Abstract The fractal nature of latex particles and their aggregates was characterised by image analysis in terms of fractal dimensions. The one- and two-dimensional fractal dimensions, D_1 and D_2, were estimated for polystyrene latex aggregates formed by flocculation in citric acid/phosphate buffer solutions. The dimensional analysis method was used, which is based on power law correlations between aggregate perimeter, projected area and maximum length. These aggregate characteristics were measured by image analysis. A two-slopes method using cumulative size distributions of aggregate length and solid volume has been developed to determine the three-dimensional fractal dimension (D_3) for the latex aggregates. The fractal dimensions D_1, D_2 and D_3 measured for single latex particles in distilled water agreed well with $D_1 = 1$, $D_2 = 2$ and $D_3 = 3$ expected for Euclidean spherical objects. For the aggregates, the fractal dimension D_2 of about 1.67 ± 0.04 ($\pm$ standard deviation) was comparable to the fractal dimension D_3 of approximately 1.72 ± 0.13 ($\pm$ standard deviation), taking the standard deviations into account. The measured three-dimensional fractal dimension for latex aggregates is within the fractal dimension range 1.6–2.2 expected for aggregates formed through a cluster-cluster mechanism, and is close to the D_3 value of about 1.8 indicated for cluster formation via diffusion-limited colloidal aggregation.

Key words Latex particles – Aggregates – Fractal dimensions – Image analysis

Introduction

Flocculation is an important mechanism of particle removal in natural and processing systems since it can transform small, slowly settling particles into large, faster settling aggregates. An understanding of the aggregate properties, such as size, shape and porosity/density, is crucial to the optimisation of solid-liquid separation processes, whether natural or industrial.

It is difficult to describe aggregate structure and characterise aggregates in terms of size, shape and/or density because of their irregular form, but this irregularity does lead itself to a fractal description. In recent years fractal geometry has been developed to describe irregular structures such as macromolecules, rivers, coastlines, mountains and clouds, and a wide range of chaotic phenomena such as turbulence and Brownian motion [1, 2]. Fractal dimension, the most important numerical parameter in the concept of fractal geometry, can be used to describe the spatial structure, i.e. how the particles occupy space in aggregates, as well as the physical properties such as porosity and/or packing density. Fractal dimensions D_n may take non-integer values (ranging between 0 and 3), which may be distinguished from the embedding dimension E and the topological dimension D_T. The embedding dimension E is the dimension of the embedding Euclidean space. In general one has [3]

$$D_T \leq D_n \leq E \quad . \tag{1}$$

Fractal geometry has proved to be a useful way of describing the highly irregular structures found in aggregated systems. Most aggregates have a non-uniform structure and the aggregate density decreases as aggregate size increases. It is generally recognised that most irreversible growth processes result in the formation of scale-invariant fractal aggregates [4]. The geometry of such aggregates can be described using the scaling relationship

$$N \propto l^{D_n} \quad , \tag{2}$$

where N is the number of the primary particles in the aggregate, D_n is the fractal dimension determined for the aggregate in n dimensions, and l is the characteristic length scale of the aggregate.

Particle collision, necessary to produce aggregates, can be generated by Brownian motion, shear, and differential sedimentation, although in practice for a given situation only one of these coagulation mechanisms is assumed to dominate, depending on particle size, temperature, and shear rate [5]. Brownian motion is generally acknowledged to be important only for small particles (≤ 1 μm); both shear and differential sedimentation have been suggested as predominating in the coagulation of particles into larger aggregates.

Two distinct, limiting regimes of irreversible colloid aggregation have been identified, and are referred to as diffusion-limited colloid aggregation (DLCA) and reaction-limited colloid aggregation (RLCA) [6]. Experiments and computer simulations of aggregation of three types of colloids indicated that two different types of aggregates could be formed as a function of particle stickiness, or differential collision efficiencies [7]. DLCA occurs when there are negligible repulsive forces between colloid particles, causing particles to stick upon contact and form highly tenuous structures. Since the probability of attachment on collision approaches unity, the aggregation rate is limited solely by particle transport. The formation of such a highly tenuous structure can be considered to be due to a very sticky particle moving in a "random walk" to the aggregate surface, with no penetration of particles into the aggregate, since they will collide with the aggregate exterior and stick there. RLCA occurs when a substantial repulsive force remains between particles, and so the attachment probability approaches zero. Particles may collide many times before sticking, allowing them to penetrate the aggregate, and so the aggregation rate is limited by the time taken for particles to overcome the repulsive barrier by thermal activation. These two regimes correspond to the limiting cases of rapid and slow colloid aggregation that have long been recognised in colloid science.

Colloidal aggregates formed by Brownian motion have been shown to be fractals [2]. There is a universality of the fractal dimensions for aggregates formed by Brownian motion, since the fractal dimensions of different colloids, such as gold, silica and polystyrene, are nearly identical when the aggregates are developed under similar conditions [7], i.e. the magnitude of fractal dimensions is independent of the details of the chemical nature of the colloid. The fractal dimension D_3 is about 1.8 for DLCA and about 2.1 for RLCA.

The magnitude of the fractal dimension is determined by the mechanism of aggregate growth, which has been demonstrated by computer simulations of aggregate growth by random processes [2]. Aggregates formed through particle-cluster mechanisms (addition of particles into the cluster one at a time) have three-dimensional fractal dimensions in the range 2.5–3.0 [8]. Most inorganic colloidal aggregates formed through collision of clusters (cluster-cluster mechanisms) have lower D_3 fractal dimensions, typically in the range 1.6–2.2 [9].

For fractal objects, the relationships between their geometric properties and their characteristic lengths can be used to determine the fractal dimension for aggregates if those properties can be measured. Since some measurable properties of fractal aggregates scale with their characteristic length according to a power law [10], the fractal dimensions can be obtained from the slopes of the logarithm of the aggregate properties and the logarithm of the aggregate characteristic length. Properties such as porosity [11], settling velocity [11, 12], and density [13] have been established for the determination of the fractal dimension for aggregates. There is a variety of methods for defining the characteristic length scale of the aggregate including longest length [11], nominal diameter [14], average of longest length in the perpendicular direction [15], longest length perpendicular to settling [16], and geometric mean and radius of gyration [7].

The aim of this work was to establish practical methods for characterising single latex particles and their aggregates formed in citric acid/phosphate buffer solutions in terms of fractal dimensions, thus enabling a better understanding of the flocculation process. The characteristic length scale is defined as the aggregate maximum length, based on image analysis, unless stated in the paper.

Materials and methods

Dimensional analysis

There are various ways and levels of precision for defining fractal dimensions. The fractal dimension D_n of aggregates is defined as the power describing how aggregate properties vary with characteristic length, in which n is the Euclidean dimension the object is embedded in, and D_n is the n-dimensional fractal dimension [1, 2].

The following relationships can be used to determine the fractal dimensions for aggregates:

$$P \propto l^{D_1} \tag{3}$$

$$A \propto l^{D_2} \tag{4}$$

$$V \propto l^{D_3} \text{ or } N \propto l^{D_3} , \tag{5}$$

where l is the aggregate maximum length, P the aggregate perimeter, A the aggregate projected area, V the solid volume, N the number of particles in the aggregate, and D_1, D_2 and D_3 are the one-, two-, and three-dimensional fractal dimensions, respectively.

Obviously the values of the fractal dimensions can be obtained from slopes of log-log plots of P, A, V, or N versus the aggregate maximum length (l). For Euclidean objects, $D_1 = 1$, $D_2 = 2$, and $D_3 = 3$. For those aggregates composed of primary particles with uniform size and density, their solid volumes are proportional to the numbers of particles in the aggregates. Computer simulations and experimental results have shown that D_3 is equal to D_2 if D_3 is less than 2 for colloidal aggregates [17]. The one-dimensional fractal dimension is of interest to discover whether it varies with changes in D_2 or D_3, since the aggregate properties that affect porosity and settling rate are only a function of D_2 and D_3 [18].

Size distribution analysis (the two-slopes method)

The three-dimensional fractal dimension D_3 can be determined from measurements of cumulative size distributions for fractal aggregates. Particle size can be described using a size distribution function $n(L)$, defined by $\mathrm{d}N = n(L)\,\mathrm{d}L$, where $\mathrm{d}N$ is the number of particles per unit volume with size in the range L to $L + \mathrm{d}L$ [19]. The characteristic length L can be any scale measure of size, e.g. diameter, volume, and maximum or average length. The cumulative size distribution $N(L)$ is commonly used, and is defined as the number concentration of particles larger than a given size L, i.e. $N(L) = \int_L^\infty n(L)\,\mathrm{d}L$ [20].

For fractal aggregates, cumulative size distributions in terms of maximum length or solid volume are given by [10]

$$N(l) = A_1 l^{S(l)} \tag{6}$$

$$N(V) = A_V V^{S(V)} , \tag{7}$$

where A_1 and A_V are empirical constants, and $S(l)$ and $S(V)$ are exponents of the cumulative size distributions $N(l)$, and $N(V)$ based on aggregate maximum length l and solid volume V, respectively. According to the definition of the cumulative size distribution, cumulative size distributions in terms of aggregate length and solid volume are equal for a given population of aggregates:

$$N(l) = N(V) . \tag{8}$$

Combining Eqs. (6)–(8) results in the following expression:

$$A_1 l^{S(l)} = A_V V^{S(V)} . \tag{9}$$

The solid volume V of the aggregate is calculated as the total volume occupied by all primary particles in the aggregate, given by [20]

$$V = \psi^{D_3/3} \delta_0 l_0^{3-D_3} l^{D_3} , \tag{10}$$

where ψ is the packing factor for aggregates, δ_0 the shape factor of the primary particles, and l_0 the length of the primary particles. Substituting Eq. (10) into Eq. (9) yields

$$A_1 l^{S(l)} = A_V \left[\psi^{D_3/3} \delta_0 l_0^{3-D_3}\right]^{S(V)} l^{S(V)D_3} . \tag{11}$$

Since the exponent of l should be the same on both sides of the above equation, one obtains

$$S(l) = D_3 S(V) , \tag{12}$$

assuming ψ does not depend on l. The fractal dimension can then be calculated from the two slopes of the cumulative size distributions in terms of maximum length and solid volume using

$$D_3 = \frac{S(l)}{S(V)} . \tag{13}$$

Theoretically, the three-dimensional fractal dimension could also be calculated using differential size distributions. However, the errors associated with fractal dimensions calculated using cumulative size distributions are less than those using differential size distributions [20]. For this reason, cumulative size distributions were used to determine D_3 in this work. Note that the fractal nature of real aggregates only applies over a restricted range of l [2].

Latex particles

Latex particles are widely used for investigating various aspects of colloidal and aggregation behaviour because of their constant size, initial monodispersivity, chemical resistance, and ability to be destabilised by salts. Latex particles are composed of a large number of polymer chains, with the individual chains having molecular weights in the range 10^5–10^7.

The particles used in this work were made of a surfactant-free zwitterionic polystyrene latex, and were purchased from the Interfacial Dynamics Corporation (Portland, Ore. USA). The single particle diameter was 1.28 μm with a standard error on the mean of $\pm 4.8\%$ (data provided by the manufacturer). The surface charge properties of latex particles depend on the pH of the medium. The isoelectric point (IEP) of the particles was known to be about 3.84, i.e. latex particles were positively charged at pH less than the IEP and negatively charged at pH greater than the IEP. Latex particles were stored in a solution of deionised water at a concentration of 4% w/w and kept cold at 4 °C.

Preparation of latex aggregates

The pH at the IEP and at a high concentration of electrolyte will cause aggregation of latex particles, since latex particles will possess zero net charge and so the electric repulsive forces between them are negligible, whilst a high electrolyte concentration will lead to an almost complete compression of the electric double layer and a reduction in the repulsive force, again promoting aggregation.

The latex aggregates were prepared by mixing a 4.0% w/w suspension of latex in distilled water with a McIlvaine buffer solution [21] using a vortex mixer for 3 s. Before mixing the latex stock suspensions had been held in an ultrasonic bath for about 20 min in order to break doublets in the suspension. The McIlvaine buffer was composed of citric acid, sodium hydrogen orthophosphate, and potassium chloride. This buffer maintained the suspensions at pH = 3.8 under an ionic strength of 1M. The final

suspensions, having a concentration of 0.1% w/v of latex, were then stored at 4 °C to prevent further aggregation that could otherwise later be caused at room temperature by Brownian motion. The preparation procedure was found to have no effect on the size distribution. Careful sampling procedures were essential during the size measurements, as the latex aggregates were very fragile.

Image analysis of latex aggregates

The fractal geometrical properties used for determining one- and two-dimensional fractal dimensions, such as perimeter, projected area, and maximum aggregate length (see Eqs. 3, 4), were obtained using an image processing and analysis system. A Quantimet 600 image analysis system (Leica Cambridge, UK) connected with a Leica DMR microscope (Leica Cambridge, UK) and a CCD video camera (model DC10.5, Sony, Japan) was used in this work. For automatic operation the microscope was fitted with a motorised stage, a controllable illumination system, and autofocus capability.

A software routine was written using the Quantimet interactive programming system and QWin (Leica's image analysis toolkit running under Microsoft Windows). This program consisted of a sequence of automatic image processing and image analysis steps executed in repeated cycles until all the selected fields of view had been analysed.

A grey image of aggregates with a resolution of 512 × 512 pixels and 256 greyness levels was captured on the image analysis computer. Such images are two-dimensional projections of aggregates in the microscope field of view. The objects (here aggregates) were detected by their greyness level. The result of this detection produced a binary image masking the part of the grey image (i.e. aggregates) of interest. As the greyness level of aggregates was not required for analysis all the subsequent image processing was on this binary image. The binary image might contain many undesired small particles and artefacts. These were selected and removed by an opening operation. Details of many image processing functions can be found in Ref. [22]. The binary image was then subjected to a closing operation in order to correct small image imperfections, mainly pixels missing from the binary image because of non-uniform intensity of the original grey image. Finally, measurements were performed on this binary image.

The aggregate maximum lengths were taken as the length of the longest feret from a series of ferets measured at 32 angles (between 0 and 180°) centred on the mass of aggregates. The aggregate perimeter was defined as the distance around the aggregate's boundaries (in the image), including those within its external perimeter, calculated by a pixel count. The projected area of an aggregate was calculated as the product of the area of a pixel and the number of the pixels within the aggregate image. All measurements were made at 40× magnification of the objective (400× overall) with a resolution of 0.165 μm using a PL Fluotar lens with a field performance of at least 25 mm.

Size distribution based on length

Size distributions in terms of length were calculated using aggregate maximum lengths, determined as described above. In order to match the size range analysed by the particle counter (described in the next section) to the satisfaction of the assumption made in the two-slopes method, aggregates with maximum lengths less than 0.7 or 2 μm corresponding to the 30 or 100 μm orifice tube used in particle counter, respectively, were excluded from the analyses.

Thousands of determinations were made so as to obtain the size distribution at a confidence level, as the size distribution is a statistical property of the population. A minimum of 1000 analysed features (objects) were accumulated for each sample by selecting viewing fields at random on the slides. A macro written for a spreadsheet under Microsoft Excel version 5.0 was used to analyse the data provided by the image analysis system, thus enabling the size distribution based on length to be obtained.

Size distribution based on solid volume

Size distributions in terms of solid volume were measured using a Coulter Multisizer II (Coulter Electronics, UK) equipped with a 30 or 100 μm orifice tube. The Coulter counter measures the number and solid volume of particles suspended in a conductive solution by counting the change in electrical current between two electrodes immersed in the conductive electrolyte on either side of a small aperture, through which a suspension of the particles is forced to flow, based on the fact that changes in solution resistance caused by the passage of a particle across the orifice tube have been found to be proportional to the solid volume of the particle.

The particle size range that the instrument can characterise depends on the orifice tube aperture diameter, i.e a size range of 0.6–18 μm and 2–60 μm corresponding to the 30 and 100 μm diameter orifice tubes, respectively. In this work, the sampling volumes were 50 and 500 μl for the 30 and 100 μm apertures, respectively. The conductive electrolytes used were Isoton II diluent (Coulter Electronics) and 1M buffer solution for single latex particle suspensions and aggregated latex suspensions, respectively. All of the buffers were filtered with a 0.45 μm cellulose acetate membrane filter. A Pentium personal computer connected to the Coulter counter was used to analyse data using the Multisizer AccuComp 1.19 software provided by Coulter, giving size distributions based on solid volume. All of the results reported here are the average of three measurements on size distribution.

Results and discussion

Validation of size measurements

The diameters of single latex particles were estimated by the Coulter counter and image analysis system to be 1.16 ± 0.13 and 1.08 ± 0.25 μm (±standard deviation), respectively, which are consistent with the value of 1.28 ± 4.8% μm (±standard error) which was provided by the manufacturer. The size distribution of single latex particles measured using the image analysis system had a similar shape to that measured using the Coulter counter (Fig. 1), indicating that these two methods give consistent results for size distribution measurements.

Fractal dimensions of single latex particles

As single latex particles can be considered to be spherical Euclidean objects, their shapes scale according to their size raised to integer powers (1 for perimeter, 2 for area, and 3 for mass or volume). For the assessment purpose, single latex particles were characterised in terms of fractal dimensions.

The perimeters of single latex particles in distilled water as a function of particle maximum length

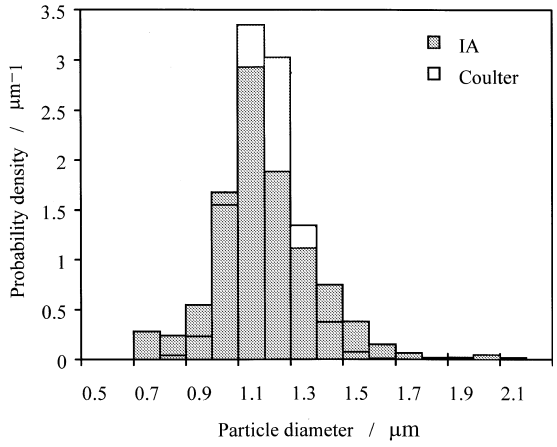

Fig. 1 Size distributions of single latex particles measured using the image analysis system and the Coulter counter

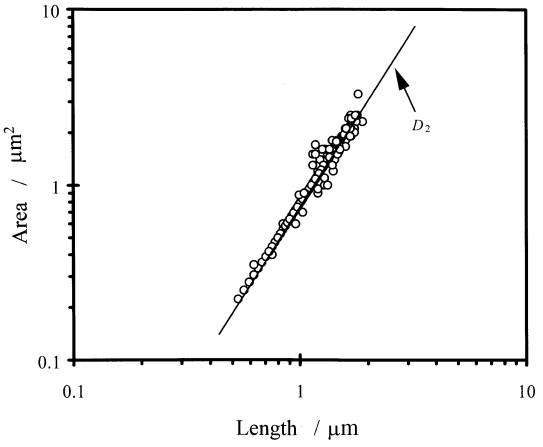

Fig. 3 Projected area of latex particles in distilled water as a function of particle length measured using the image analysis system

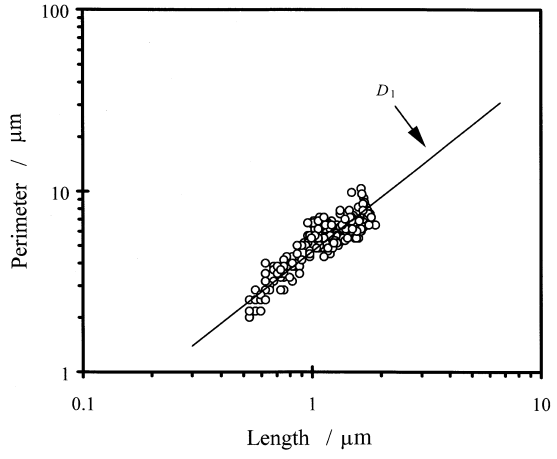

Fig. 2 Latex particle perimeter as a function of particle length in distilled water measured using the image analysis system

measured using the image analysis system are shown in Fig. 2. The maximum lengths of single latex particles were identical to their diameters as expected for spherical particles. From a log-log regression of Eq. (3), the one-dimensional fractal dimension D_1 was estimated to be 1.06 ± 0.07 (± standard deviation) for single latex particles, which is close to the Euclidean value of $D_1 = 1$ expected for spherical particles. It is noted that all of the measurements were taken within 10 min for each sample in order to minimise the formation of latex aggregates due to Brownian motion at room temperature.

The projected areas of single latex particles in distilled water as a function of particle length measured using the image analysis system are shown in Fig. 3. A total of 1000 latex particles ranging from 0.5 to 2 μm were used to calculate the two-dimensional fractal dimension of $D_2 = 2.01 \pm 0.03$ (± standard deviation) from a log-log plot of length and projected area according to Eq. (4). This value is identical to the Euclidean value of $D_2 = 2$ expected for spherical particles and is experimental evidence of the spherical structure of the latex particles.

The comparisons of projected area A and perimeter P can provide structural information on single latex particles. Perfectly spherical particles should appear in projection as circles during image analysis and processing [22], for which the following isometric relationships can be derived:

$$A = P^2/4\pi \tag{14}$$

or

$$\log(A) = \log(1/4\pi) + 2\log(P) \ . \tag{15}$$

The slope of the log-log plot of perimeter and area (Fig. 4) was estimated to be 1.96, which is comparable to the value of 2 expected for spherical particles; and the intercept value of −1.16 is close to −1.10 [$= \log(1/4\pi)$], both implying that latex particles in distilled water have a relatively low surface roughness.

The two slopes from the size distributions in terms of length and solid volume were used to calculate the three-dimensional fractal dimension of single latex particles. The cumulative size distribution based on length for latex particles in distilled water measured using the image analysis system is shown in Fig. 5. From the log-log plot of number and length, based on Eq. (6), the slope $S(l)$ was determined to be 11.49 with respect to the size ranging from 1 to 2 μm. Similarly, the slope of the log-log plot of cumulative number and solid volume, $S(V) = 3.80$, was obtained for latex particles from Fig. 6 in the length range of 1–2 μm according to Eq. (7). The two slopes $S(l)$ and $S(V)$

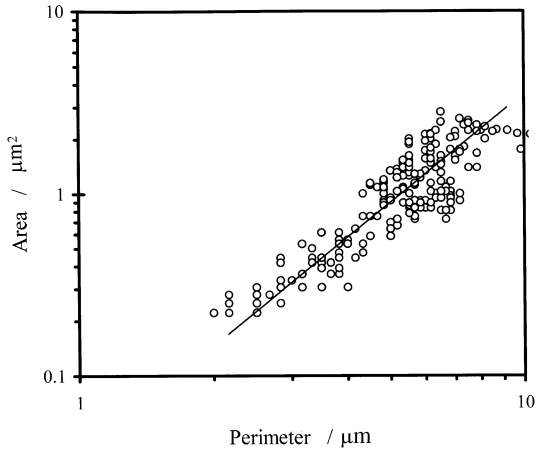

Fig. 4 Plot of projected area against perimeter for latex particles in distilled water

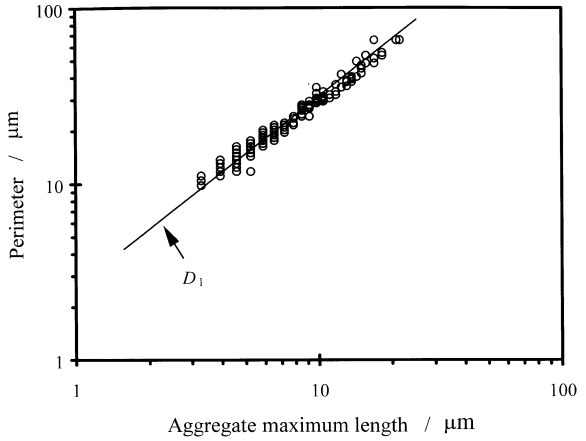

Fig. 7 Aggregate perimeter as a function of aggregate maximum length measured using the image analysis system for latex aggregates formed in 1M McIlvaine buffer solution

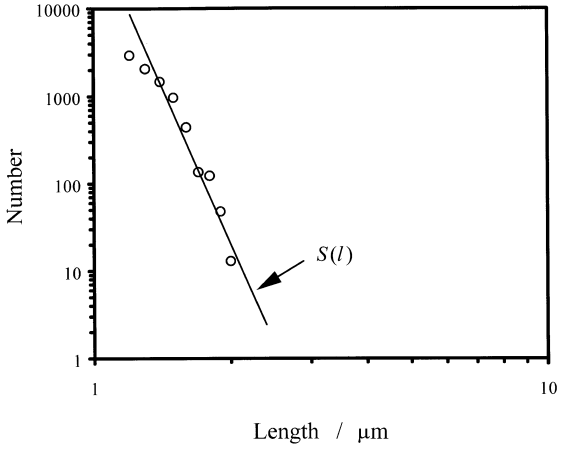

Fig. 5 Cumulative size distribution of latex particles in distilled water measured using the image analysis system

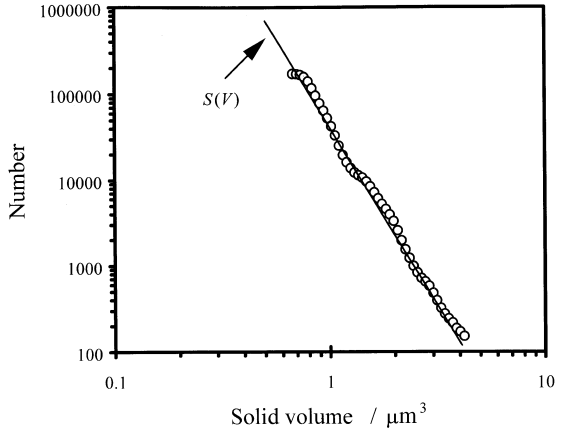

Fig. 6 Cumulative size distribution of latex particles in distilled water measured using the Coulter counter

from the size distributions for the same range of latex particle diameter were used to calculate the fractal dimension, giving $D_3 = 3.02 \pm 0.08$ ($\pm$standard deviation).

The fractal dimensions of single latex particles were nearly identical to the Euclidean dimensions $D_1 = 1$, $D_2 = 2$, and $D_3 = 3$ expected for spherical objects, implying that the latex particles in distilled water are spherical Euclidean objects and that the measurement methods for determining fractal dimensions are reliable.

Fractal dimensions of latex aggregates from dimensional analysis

The power-law relationships between aggregate perimeter or projected area and aggregate characteristic length described in the materials and methods section were used to determined one- and two-dimensional fractal dimensions of the latex aggregates. The aggregate maximum length was chosen as the aggregate characteristic length scaling with aggregate properties, as it was not possible to determine the relative position of each particle in the aggregates.

The aggregate perimeters as a function of aggregate maximum length measured using the image analysis system for latex aggregates formed in 1M McIlvaine buffer solution are shown in Fig. 7. The aggregate perimeter scaled with the aggregate maximum length according to a power law with an exponent of 1.04, indicating that the one-dimensional fractal dimension of latex aggregates is $D_1 = 1.04 \pm 0.08$ ($\pm$standard deviation). This value is comparable to the one-dimensional fractal dimension of single latex particles in distilled water (see the previous section), and is also close to the value of $D_1 = 1.0$ expected for Euclidean spherical

objects. However, it would not imply that latex aggregates formed in the buffer behave as Euclidean objects, as not only the fractal structures of latex aggregates were observed during the image analysis, but also one-dimensional fractal dimensions have been reported not to correlate to the trends in two- or three-dimensional fractal dimensions for marine snow aggregates [23].

As the one-dimensional fractal dimension accesses how the aggregate perimeter changes with aggregate length, it is sensitive to the irregularity of the boundary of the aggregates. The similarity of the boundary fractal dimensions has been previously found for all groups of marine snow aggregates [23], although the dimensions did have significantly different magnitudes of D_2 and D_3, implying that it would not be possible to distinguish between different types of aggregates based only on boundary fractal dimension or one-dimensional fractal dimension.

The aggregate projected areas as a function of aggregate maximum length measured using the image analysis system for latex aggregates formed in 1M McIlvaine buffer solution are shown in Fig. 8. A two-dimensional fractal dimension of $D_2 = 1.67 \pm 0.04$ ($\pm$standard deviation) was obtained from the slope of log-log plots in Fig. 8 based on analysis of more than 2000 aggregates for each measurement. This value is significantly smaller than the value of $D_2 = 2$ expected for Euclidean spherical aggregates even when taking the standard deviation into account, which is experimental evidence of the two-dimensional fractal structure of the latex aggregates formed in the buffer solutions. Since the same samples were used to determine D_1 and D_2 by the image analysis system, a lack of correlation between trends in D_1 and D_2 fractal dimensions indicates that the fractal nature of the aggregate perimeter was not correlated with changes in aggregate area for the latex aggregates.

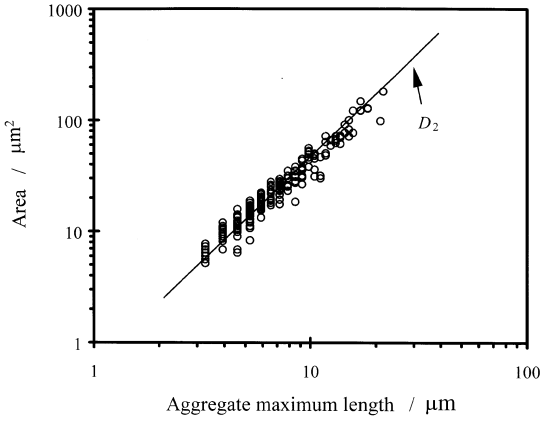

Fig. 8 Aggregate area as a function of aggregate maximum length measured using the image analysis system for latex aggregates formed in 1M McIlvaine buffer solution

Fractal dimensions of latex aggregates from size distributions

The two-slopes method based on size distributions was used to determine the three-dimensional fractal dimension of latex aggregates. The cumulative size distribution of latex aggregates formed in 1M McIlvaine buffer solution in terms of maximum length measured using the image analysis system is shown in Fig. 9. The size distribution curve was not completely linear over the whole size range: the linear part corresponds to a size range of 4–18 μm that covers 95% of the size distribution of the latex aggregates as shown in Fig. 10. Hence, a slope of $S(l) = 2.15 \pm 0.15$, derived from the log-log plot of cumulative number and aggregate maximum length, was obtained for the latex aggregates in the maximum length range of 4–18 μm.

The slope $S(V)$ based on size distribution in terms of solid volume was obtained from the log-log plot of cumulative number and aggregate solid volume measured using the Coulter counter as shown in Fig. 11,

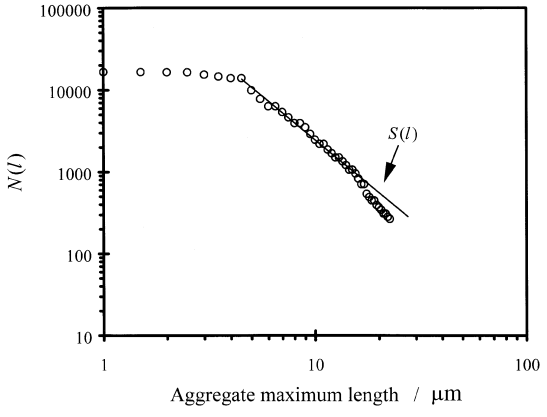

Fig. 9 Cumulative size distribution of latex aggregates formed in 1M McIlvaine buffer solution in terms of maximum length measured using the image analysis system

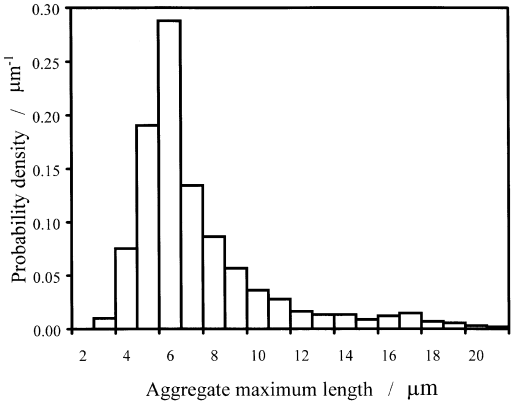

Fig. 10 Size distribution of latex aggregates formed in 1M McIlvaine buffer solution measured using the image analysis system

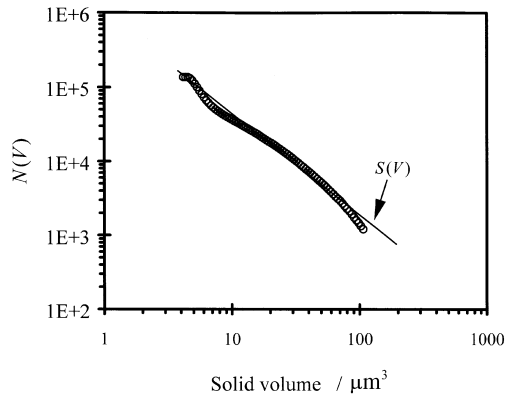

Fig. 11 Cumulative size distribution of latex aggregates formed in 1M McIlvaine buffer solution in terms of solid volume measured using the Coulter counter

giving $S(V) = 1.25 \pm 0.06$. This standard deviation was slightly smaller than that for size distribution measurements in terms of length, possibly due to the instruments themselves. Dividing $S(l)$ by $S(V)$ yields a fractal dimension of $D_3 = 1.72 \pm 0.13$ ($\pm$standard deviation) for latex aggregates, which is significantly smaller than the value of $D_3 = 3$ expected for Euclidean spherical objects and is again experimental evidence of the three-dimensional fractal structure of latex aggregates formed in the buffer solutions.

The error of the calculated three-dimensional fractal dimension is slightly higher than those of the one- and two-dimensional fractal dimensions for latex aggregates, because the error in D_3 comes from the standard deviations of two slopes, whereas errors in D_2 and D_1 were referred only to the standard deviation of one slope. The values and standard deviations of D_3, $S(l)$, and $S(V)$ for latex aggregates formed in 1M McIlvaine buffer solutions are summarised in Table 1. Obviously fractal dimensions calculated from the size distributions are very sensitive to the errors in slopes, i.e. errors in defining the size range that describes the same set of aggregates for determining $S(l)$ and $S(V)$.

According to fractal mathematics, the D_3 fractal dimension should be equal to the D_2 fractal dimension if

Table 1 Three-dimensional fractal dimensions D_3 of latex aggregates

$S(l)$	$S(V)$	D_3			
2.29	1.27	1.80	1.94	1.85	1.73
2.38	1.18	1.87	2.02	1.92	1.80
2.04	1.24	1.61	1.73	1.65	1.55
2.01	1.32	1.58	1.70	1.62	1.52
2.08		1.64	1.76	1.68	1.58
2.12		1.67	1.80	1.71	1.61
2.15 ± 0.15[a]	1.25 ± 0.06[a]	1.72 ± 0.13[a]			

[a] Denotes mean value $\pm$ standard deviation

D_3 is less than 2 [17]. The three-dimensional fractal dimension D_3 of latex aggregates formed in the buffer solutions was slightly higher than the D_2 fractal dimension, and this discrepancy may have arisen from the two different methods of calculating D_3 and D_2. However, D_3 is comparable to D_2 when taking the standard deviations into account.

Implications of fractal dimensions for flocculation

Fractal dimensions access how aggregate geometric properties change with aggregate characteristic length. The closer D_1, D_2, and D_3 are to 1, 2, and 3 that are expected for Euclidean objects, respectively, the more the aggregate scales like an ordinary Euclidean object. The two-dimensional fractal dimension should not exceed 2 since the projected area of aggregates cannot grow at a faster rate than the square of aggregate maximum length ($D_2 \leq 2$). Similarly, D_3 should not be greater than 3 as the dimension of embedding Euclidean space for aggregates is 3.

Since fractal dimensions characterise how aggregate properties change with size, their magnitude is related to the aggregate morphology. Aggregates with highly irregular perimeters have one-dimensional fractal dimensions greater than unity; D_1 increases with the irregularity of the boundaries of aggregates. Aggregates tend to become more porous with increasing size, resulting in D_2 and D_3 fractal dimensions that are less than 2 and 3, respectively. The lower D_2 and D_3 indicate that aggregates are more amorphous and less compact, whereas aggregates that are more compact should have higher D_2 and D_3 fractal dimensions.

The magnitude of the fractal dimension could be used to estimate the aggregation mechanism. The measured three-dimensional fractal dimensions of latex aggregates are within the fractal dimension range 1.6–2.2 expected for aggregates formed through a cluster-cluster mechanism during aggregate growth, and are close to the D_3 value of about 1.8 indicated for cluster formation via DLCA. This further supports the observation that there is a universality in colloid aggregation with respect to the fractal dimension, i.e. the magnitude of the fractal dimension is independent of the type of colloid [7]. The highly tenuous structures of latex aggregates observed during image analysis is a result of very sticky particles moving in a random walk, and is also experimental evidence of cluster formation by diffusion-limited aggregation, since latex aggregates formed by Brownian motion as expected from the experimental procedure.

Conclusions

The dimensional analysis method based on fractal power laws using image analysis provided a useful technique

for determining one- and two-dimensional fractal dimensions for latex aggregates. The two-slopes method based on cumulative size distributions in terms of aggregate length and solid volume has been used to measure the three-dimensional fractal dimension D_3 of latex aggregates with an estimated error of 8%.

The one-dimensional fractal dimension is probably not useful as a basis for distinguishing between different types of aggregates. A more useful application of the two- and three-dimensional fractal dimensions (D_2 and D_3) may be as a tool to understand how morphology and aggregate properties, such as density, porosity, and size, vary under different culture conditions (such as shear force and sedimentation).

Fractal dimensions should facilitate understanding of morphology and of properties of aggregates. However, there may be many factors that affect the ability to model the overall coagulation and sedimentation processes using fractal geometry, such as coagulant dosage, ionic strength, pH, shear field (laminar and turbulent), and mixing conditions.

Acknowledgements The authors would like to thank Graham P. McCauley for useful discussions. Funding was provided by BBSRC.

References

1. Feder J (1989) Fractals. Plenum, New York
2. Pfeifer P, Obert M (1989) In: Avnir D (ed) The fractal approach to heterogeneous chemistry: surfaces, colloids, polymers. Wiley, New York, pp 11
3. Harrison A (1995) Fractals in chemistry. Oxford University Press, Oxford
4. Ayazi Shamlou, Titchener-Hooker N (1993) In: Ayazi Shamlou (ed) Processing of solid-liquid suspensions. Butterworth Heinmann, London, pp 1
5. Hunt JR (1982) J Fluid Mech 122:303
6. Weitz DA, Huang JS, Lin MY, Sung J (1985) Phys Rev Lett 54:1416
7. Lin MY, Lindsay HM, Weitz DA, Ball RC, Klein R, Meakin P (1989) Nature 339:360
8. Schaefer DW (1989) Science 243:1023
9. Witten TA, Cates ME (1986) Science 232:1607
10. Jiang Q, Logan BE (1996) J Am Water Works Assoc 88:100
11. Logan BE, Wilkinson DB (1991) Biotechnol Bioeng 38:389
12. Li DH, Ganczarczyk JJ (1989) Environ Sci Technol 23:1385
13. Logsdon SD (1995) Soil Sci Soc Am J 59:1216
14. Mueller JA, Morand J, Boyle WC (1967) Appl Microbiol 15:40
15. Davis RH, Hunt TP (1986) Biotechnol Prog 2:91
16. Alldredge AL, Gottschalk C (1988) Limnol Oceanogr 33:339
17. Meakin P (1988) Adv Colloid Interface Sci 28:249
18. Jiang Q, Logan BE (1991) Environ Sci Technol 25:2031
19. Hunt JR (1980) In: Kavanaugh MC, Leckie JO (eds) Particles in water. Adv Chem Ser 189. American Chemical Society, Washington, D.C. p243
20. Logan BE, Kilps JR (1995) Water Res. 29:443
21. Elving PJ, Markowitz JM, Rosenthal I (1956) Anal Chem 28:1179
22. Paul GC, Thomas CR (1998) In: Schügerl K (ed) Relation between morphology and process performance. Advances in biochemical engineering/biotechnology. Vol. 60, Springer-Verlag, Berlin, p 1
23. Kilps JR, Logan BE, Alldredge AL (1994) Deep-Sea Res 41:1159